

Magnetic resonance cholangiography:
comparison of two- and three-
dimensional sequences for assessment
of malignant biliary obstruction

Jin-Young Choi

Department of Medicine

The Graduate School, Yonsei University

Magnetic resonance cholangiography:
comparison of two- and three-
dimensional sequences for assessment
of malignant biliary obstruction

Jin-Young Choi

Department of Medicine

The Graduate School, Yonsei University

Magnetic resonance cholangiography:
comparison of two- and three-
dimensional sequences for assessment
of malignant biliary obstruction

Directed by Professor Myeong-Jin Kim

The master's Thesis submitted to the Department of
Medicine, the Graduate School of Yonsei University in
partial fulfillment of the requirements for the degree of
Master of Medicine

Jin-Young Choi

June 2006

This certifies that
the Master's Thesis of
Jin-Young Choi is approved

Thesis Supervisor : Myeong-Jin Kim

Woo Jung Lee

Yong-Min Huh

The Graduate School
Yonsei University

June 2006

Acknowledgement

There have been a number of people without whom this thesis could not be completed. My deepest gratitude goes out to Professor Myeong-Jin Kim. He sometimes gave many academic guidance and discipline as a professor not to be drowned to an error, and sometimes gave me a big smile and encouragement as a senior whenever I suffer hardship during my work.

Especially I would like to thank my committee members: Professor Woo Jung Lee and Yong-Min Huh for their perceptive comments and persistent efforts to help me make good thesis. I thank Dr. Jeong Min Lee, Dr. Jae Young Lee, Dr. Se Hyung Kim, and Dr. Joon Koo Han for help me complete this thesis in reviewing the images, data collection, and comments. I also thank Dr. Ki Whang Kim and Dr. Byung Ihn Choi who inspired me to strive for excellence.

I would like to express my infinite gratitude to my dear wife who gave me unchanged applause and encouragement. I wish to thank my parents and parents-in-law, who always help me physically and spiritually.

Written by Jin-Young Choi

Contents

Abstract	1
I. Introduction	3
II. Materials and Methods	5
1. Patient selection	5
2. Examination technique	6
3. Image analysis	9
4. Statistical analysis	11
III. Results	13
IV. Discussion	30
V. Conclusion	34
References	35
Abstract (in Korean)	38

LIST OF FIGURES

Figure 1. 2D and 3D MRC showing overall image quality ..	14
Figure 2. 2D and 3D MRC of a hilar cholangiocarcinoma.....	16
Figure 3. 2D and 3D MRC of a hilar cholangiocarcinoma underestimated for the extent of tumor.....	18
Figure 4. 2D and 3D MRC showing origin of the tumor	27

LIST OF TABLES

Table 1. Evaluation of image quality, artifact, ductal conspicuity	13
Table 2. Accuracy of 2D-MRC versus 3D-MRC for determining tumor extent according to the final diagnosis	23
Table 3. AUC (area under the curve) of extent of the disease according to the location	24
Table 4. Sensitivity, specificity, and accuracy of 2D-MRC and 3D-MRC according to the location of obstruction	25
Table 5. Interobserver agreement in the level of confidence in the evaluation of tumor extent	29

Abstract

Magnetic resonance cholangiography: comparison of two- and three-dimensional sequences for assessment of malignant biliary obstruction

Jin-Young Choi

**Department of Medicine,
The Graduate School, Yonsei University**

(Directed by Professor Myeong-Jin Kim)

The purpose of this study was to compare two-dimensional (2D) MR cholangiography (MRC) including breath-hold single-shot rapid acquisition with relaxation enhancement (RARE) and multislice half-Fourier RARE versus navigator-triggered 3D RARE MRC for the evaluation of biliary malignancy.

The MRC findings were evaluated in 31 patients with malignant biliary obstruction. Pathologic diagnoses included biliary malignancy, gallbladder carcinoma, and ampullary cancer. Two observers independently reviewed the images in a blinded fashion to assess the overall image quality, artifacts, ductal conspicuity, extent of disease, diagnostic confidence of tumor extent, and origin of the tumor. The results of MRC were compared with the definitive diagnosis, which was based on the surgical and histopathologic findings.

Studies obtained with 3D-MRC were of significantly higher technical quality than those obtained with 2D-MRC. The accuracy between two sequences for classification of the tumor was 67.7% (21 of 31), 70.9% (22 of 31) for 2D-MRC and 74.1% (23 of 31), 77.4% (24 of 31) for 3D-MRC, which was not statistically significant. There was no significant difference between the

Az values of the 2D- and the 3D-MRC for overall tumor extent in right and left second order branch, intrapancreatic CBD involvement (Az = 0.889, 0.881 for 2D and Az = 0.903, 0.864 for 3D). There was no significant difference between 2D-MRC and 3D-MRC in the assessment of origin of the tumor ($P>0.05$).

Although 3D-MRC has superior image quality to 2D-MRC, 3D-MRC showed no difference in accuracy compared with 2D-MRC for evaluating the extent of disease in malignant biliary obstruction.

Key words : magnetic resonance cholangiography; three dimensional; malignant biliary neoplasm

Magnetic resonance cholangiography: comparison of two- and three-dimensional sequences for assessment of malignant biliary obstruction

Jin-Young Choi

**Department of Medicine,
The Graduate School, Yonsei University**

(Directed by Professor Myeong-Jin Kim)

I. Introduction

Malignant biliary obstruction present as obstructive jaundice or cholangitis in many patients. The causes of malignant biliary obstruction are primary the bile duct cancer or secondary involvement of the biliary tree by extension from primary or metastatic tumors of the liver, gallbladder, or adjacent lymph nodes ¹. The goals of radiologic procedure in malignant biliary obstruction are to confirm the presence of biliary obstruction, its location, extent, and probable cause ². The accurate evaluation of location and extent of the tumors are crucial because these determine resectability and choice of the treatment modality. Although direct cholangiography including endoscopic retrograde cholangiography (ERC) and percutaneous transhepatic

cholangiography (PTC) remains the standard of reference for visualizing the presence and level of the obstruction, this technique is operator dependant and is associated with considerable complication rate ³⁻⁵.

MR cholangiography (MRC) is an evolving noninvasive and highly accurate method of imaging the biliary tree ^{3,6-11}. MRC techniques use T2-weighted sequences to depict the fluid within the biliary ductal system as high signal intensity. Current MRC techniques typically utilize thick section single-shot rapid acquisition with relaxation enhancement (RARE) and thin section half-Fourier RARE techniques to produce images of the biliary tree ^{2,12}. The two-dimensional (2D) thick section RARE technique usually consists of a single T2-weighted image (usually 30-80 mm in section thickness) acquired in the coronal and oblique coronal planes. Thin section half-Fourier RARE techniques are performed with slice thickness of 4-6 mm and subsequent maximum-intensity-projection (MIP) postprocessing. These techniques have inherent limitation of low signal-to-noise ratio (SNR) and contrast resolution ^{2,12,13}.

It is well-known that 3D RARE technique have advantage over 2D imaging to enable operator independent imaging, large-volume coverage, thinner sections without interslice gaps and a higher SNR ¹⁴⁻¹⁷. Its ability of data reformation and volume rendering has the potential to clarify anatomic relationships. There have been reports that 3D RARE MRC can provide similar

visualization rate for bile duct compared to conventional 2D techniques^{18,19}. However, there has been no study comparing 2D and 3D-MRC in patients with malignant biliary obstruction.

The purpose of this study was to compare 2D RARE MRC (breath-hold thick section single-shot RARE and multislice half-Fourier RARE) and navigator-triggered 3D RARE MRC for the evaluation of biliary malignancy.

II. Materials and Methods

Patient selection

The institutional review board approved this retrospective study and waived the requirement for informed consent. Between January 2004 and October 2005, we identified patients with a diagnosis of biliary malignancy and who received surgical treatment at our institution from a database maintained by the hepatobiliary section of the department of surgery and from pathologic reports. Criteria for inclusion of patients were as follows: patients with malignant biliary obstruction who had undergone surgical resection at our institution; patients had undergone preoperative imaging with MRC; and diagnosis of adenocarcinoma at pathologic examination of surgically resected tumor. Of the 83 patients (50 men and 33 women) initially found, 52 were excluded from the study for any of the following reasons: (a) peripheral

cholangiocarcinoma (n= 24); (b) incomplete surgical evaluation and pathologic examination due to peritoneal seeding at laparotomy (n= 5); and (c) patients who underwent biliary drainage before surgery (n= 23).

Therefore our retrospective study population included 31 patients (21 men, 10 women) with an age range of 47 to 86 (mean; 63.5) years. The presenting symptoms were jaundice (n=24), abdominal pain (n=3), general weakness (n=2), weight loss (n=1), and incidentally found mass on ultrasonography (n=1). Clinical suspicion of pancreaticobiliary duct in patients without jaundice was aroused by elevated levels of liver enzymes (n=4) or by CT with abnormal findings (n=3).

Examination Techniques

MRCP examinations were performed with a 1.5-T MR imaging system (Magnetom Sonata; Siemens, Erlangen, Germany). A phased-array body coil with four elements was used. No medication or contrast medium was administered prior to imaging. Three different MRCP sequences, 2D thick section RARE technique, thin section half-Fourier RARE technique, and navigator-triggered isotropic 3D MRCP using turbo spin echo (TSE) were applied as part of the comprehensive MR imaging examination typically performed in patients with biliary obstruction.

2D thick section RARE technique MRCP

The thick section RARE images were obtained at five oblique coronal angles (-15°, -25°, 0°, 15°, 25°) to allow optimal visualization of the bile ducts. The parameters for thick section RARE imaging were as follows: TR (repetition time, msec)/TE (effective echo time, msec), 2800/1100; echo train length, 240-256; flip angle for refocusing pulse 150° ; slab thickness, 60-80 mm; field of view, 206 X 220 mm; matrix, 240 X 256; orientation, oblique coronal planes (-15°, -25°, 0°, 15°, 25°); 5 short breath holds; acquisition time per image, 3 seconds.

Thin section half-Fourier RARE techniques

Thin section half-Fourier RARE images were obtained in coronal and axial planes. The parameters for thin section half-Fourier RARE imaging were as follows: TR (msec)/TE (msec), 1200/84-120; echo train length, 256; flip angle for refocusing pulse 150°; slice thickness, 3 mm; no gap; field of view, 280-370 mm; matrix, 256 X 218; single breath hold; and acquisition time, 18-22 seconds. Fat saturation was used to reduce strong fat signal during image acquisition. Maximum-intensity-projection postprocessing was performed.

Navigator-triggered isotropic 3D MRCP using turbo spin echo (TSE)

The acquisition parameters for 3D-MRC included the following: TR (msec)/TE (msec)/flip angle, 1100-1700/545-677; matrix size, 320 x 320; slab thickness, 60 mm; section thickness 1.0 mm; field-of-view, 320 x 315 mm; 60 partitions with interpolated partition thickness, 1 mm; typical voxel size 1mm X 1mm X 1mm; coronal orientation; parallel acquisition technique (PAT) factor 2; and minimum scan time 5 min.

Respiratory monitoring was done using navigator echoes. The navigator column was formed by a spin echo at the intersection of two oblique slices each 10 mm thick, using flip angles of 90 and 180°. The navigator column was oriented to capture the diaphragm-lung border and positioned central on the diaphragm. The underlying navigator sequence of the 3D TSE is a TSE sequence with a very low resolution in the phase encoding direction, continuously acquiring a coronal gradient echo image representing the current position of the diaphragm. Navigator echoes were acquired before and after each segment. If the diaphragm-lung border was within the selected acceptance window before and after each segment, the data collected during the segment was accepted. Otherwise, the data was rejected and reacquired. The actual scan time varied with respiratory rate but averaged about 7 to 8 min. Rotating MIP reconstructions of the 3D-MRC data were performed at a workstation (Syngo

Leonardo; Siemens) to produce images rotating about the z- and x-axis in 5° increments.

Image analysis

Two abdominal radiologists (S.H.K., J.Y.L.) reviewed all MRC images retrospectively by using a picture archiving and communication system (PACS; Marotech, Seoul, Korea) workstation monitor; the radiologists' experiences with MRC were six and eight years respectively. MRC images were initially stored on and retrieved from the PACS system. All cases were reviewed randomly and without knowledge of clinical data. Neither retrospective reader was involved in the prospective clinical interpretation of images. The two reviewers first reviewed the 2D thick section and multislice thin section MRC images. For comparison of the overall image quality, artifacts, ductal conspicuity of the sequence, they graded the 2D thick section MRC, 2D thin section MRC rotating MIP reconstruction. For the comparison of extent of the disease and origin of the tumors, they assessed the 2D-MRC including thick section-, thin section RARE sequences (axial and coronal source images). The reviewers were given a list of case (patient) numbers in random order and reviewed the 2D-MRC images respectively. And then, the readers reviewed the 3D-MRC including source images and rotating MIP reconstruction for evaluation of the overall

image quality, artifacts, ductal conspicuity, assessment of extent of the disease and origin of the tumor using the same method used for review of 2D-MRC. To avoid any bias from reviewers' memory of findings on other sequences, review of each MRC was performed with 2 weeks interval.

They graded the overall image quality using a four-point scale system from 1 to 4 (1= non-diagnostic; 2= poor quality; 3= good quality; 4= excellent quality). Artifacts were graded into four categories: 1, none; 2, minimal; 3, present but not affecting the diagnostic evaluation; 4, present and affecting the diagnostic evaluation. The reviewers were asked to record the degree of ductal conspicuity using a four-point scale from 1 to 4 (1= not-visible; 2= poor; 3= good; 4= excellent). The good quality was defined as intrahepatic ducts are clearly visualized regardless of pancreatic duct visibility.

Each reviewer assessed the extent of disease according to the diagnostic criteria (loss of continuity of bile duct, an abrupt and irregular narrowing of a distal segment with prestenotic dilatation, and irregularly shaped intraluminal filling defects). We classified the lesions into hilar and common bile duct (CBD) obstruction according to the location of the tumor. The hilar duct obstruction was determined by Bismuth and Corlette classification ²⁰. The CBD obstruction was classified into involvement of the intrapancreatic CBD and extrapancreatic CBD because intrapancreatic CBD involvement by tumor

lead to pancreaticoduodenectomy. The reviewers recorded the classification of the tumors according to the anatomical location.

They used a five-point scale to rate their confidence in evaluating the extent of disease: 1, definitely not involved; 2, probably not involved; 3, possibly involved; 4, probably involved; 5, definitely involved by tumor. The confidence rating was done for three anatomic site; right second order branch duct, left second order branch duct, and intrapancreatic CBD, respectively. For example, the reviewers recorded their confidence 5 for right second order branch duct, 2 for left second order branch duct, and 1 for intrapancreatic CBD, respectively in case of Bismuth type 3a cholangiocarcinoma. The reviewers were aware that for statistical analysis purposes, only scores of 4 and 5 would be considered as indicating tumor involvement. The reviewers also asked to record the origin of the tumors.

Statistical analysis

A *P* value of less than 0.05 was considered to be indicative of a statistically significant difference.

Image quality.- Overall image quality, artifact, ductal conspicuity of 2D thick section MRC, 2D thin section MIP and 3D- MRC rotating MIP reconstruction were compared by Friedman test.

Extent of disease.- Receiver operating characteristic (ROC) curve analysis was performed to compare the assessment of tumor extent in each portion (right second order branch, left second order branch, and intrapancreatic CBD) for the 2D-MRC images versus the 3D-MRC images. Binormal ROC curves were fitted using the MedCalc program (version 6.15.000; MedCalc Software, Mariakerke, Belgium). The diagnostic capability was determined by calculating the area under the ROC curve (A_z) for each reviewer. Calculation of the statistical significance of the difference between the areas under the ROC curves of the 2D-MRC and 3D-MRC, was performed using the univariate z score test using the same software. Sensitivity, specificity, and accuracy were calculated as follows: sensitivity = $(TM/PT) \times 100$, where TM is the number of correct tumor involvement on MRC and PT is the number of proved tumor involvement; specificity = $(NT/PN) \times 100$, where NT is the number of correct diagnosis of noninvolvement by tumor on MRC and is the number of proved noninvolvement by tumor; and accuracy = $[(TM + NT)/(PT + PN)] \times 100$.

Interobserver agreement.- To measure the agreement between two sequences and between the reviewers in the level of confidence in evaluation of tumor extent, weighted κ values were calculated. A weighted κ value less than 0.20 was considered to indicate poor agreement; a κ value of 0.20–0.39, fair agreement; a κ value of 0.40–0.59, moderate agreement; a κ value of 0.60–

0.79, substantial agreement; and a κ value of 0.80 or greater, excellent agreement.

III. Results

Image quality

Results of the comparison of overall image quality, artifacts, and ductal conspicuity are displayed in Table 1.

Table 1. Evaluation of image quality, artifact, ductal conspicuity

	RARE		HASTE		3D	
	Reviewer 1	Reviewer 2	Reviewer 1	Reviewer 2	Reviewer 1	Reviewer 2
Image quality	2.51±0.85	2.80±0.65	3.16±0.58	2.64±0.55	3.61±0.49	3.38±0.61
Artifact	1.74±0.59	1.77±0.66	2.93±0.35	1.87±0.67	1.67±0.59	1.48±0.62
Ductal conspicuity	3.16±0.49	2.96±0.61	3.38±0.52	2.70±0.64	3.77±0.49	3.61±0.61

Data are mean \pm standard deviation.

For both reviewers, the overall image quality of 3D-MRC was judged to be higher than that of corresponding 2D thick section RARE and thin section RARE MRC (Fig.1). *P* values obtained with Friedmann test demonstrated these differences to be statistically significant for both reviewers (*P* <0.05 for reviewer 1, *P* <0.001 for reviewer 2).

Figure 1. 76-year-old female with mid common bile duct cancer.

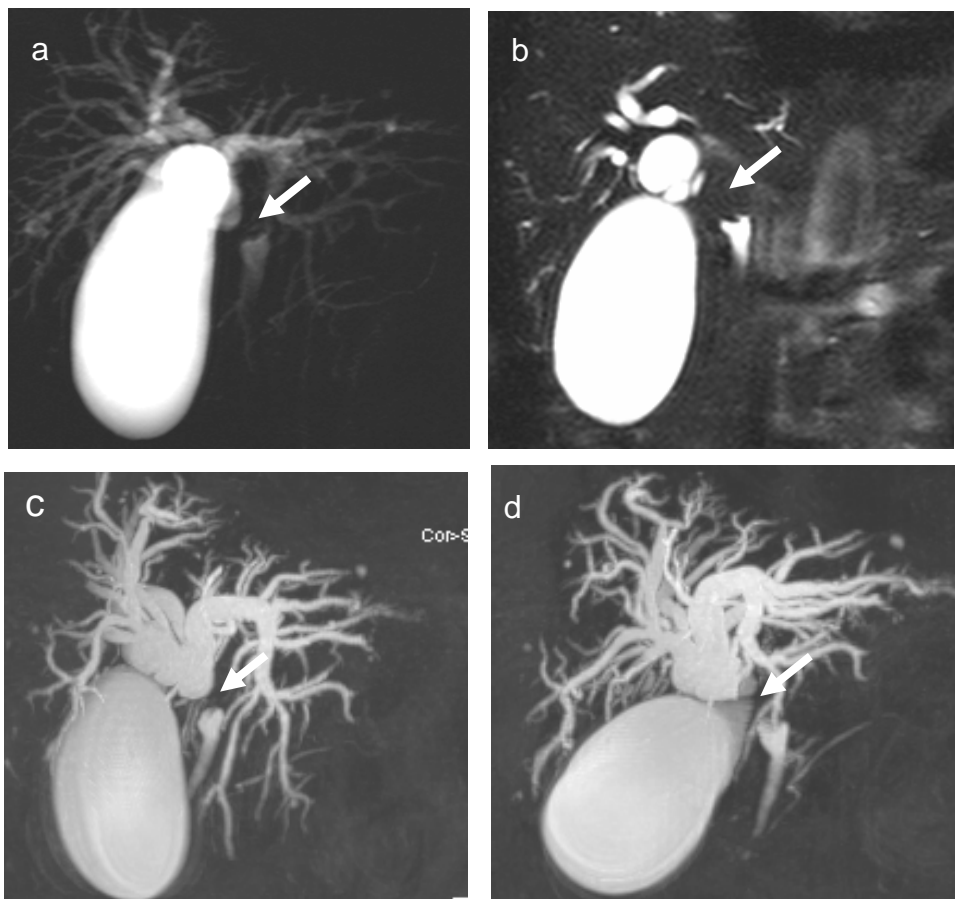
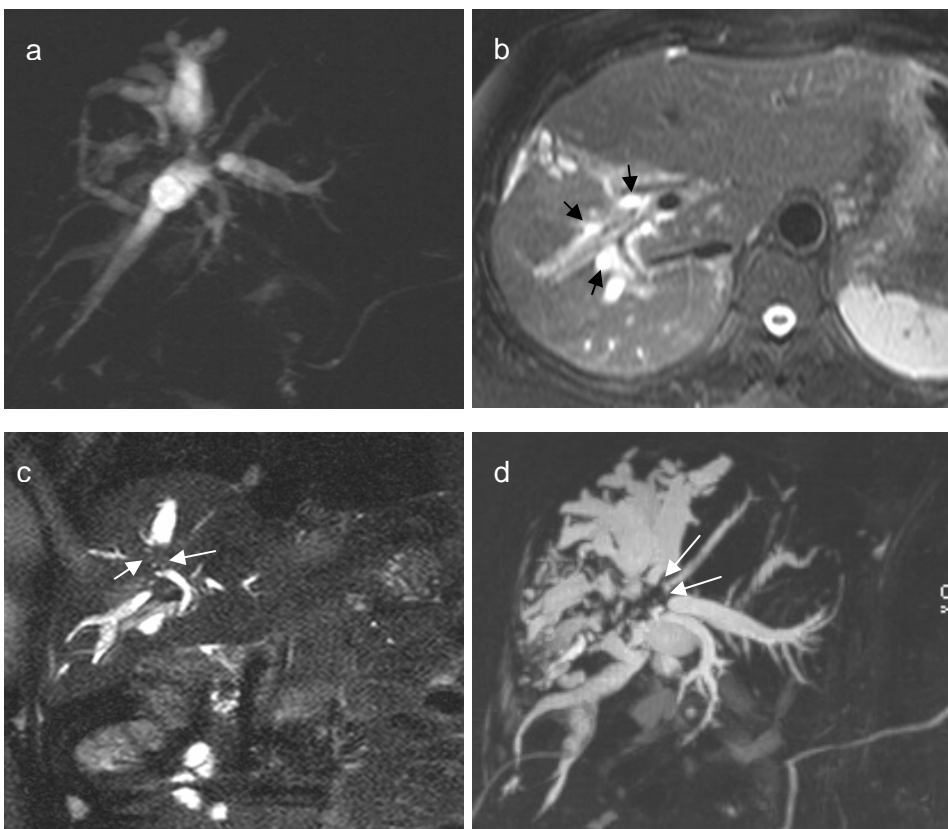


Figure 1. 76-year-old female with mid common bile duct cancer. (a) Two-dimensional (2D) thick section RARE image shows abrupt narrowing of the mid common bile duct (arrow) and bilateral intrahepatic duct (IHD) dilatation. (b) 2D thin section multislice RARE image demonstrates the mid CBD obstruction (arrow). (c)(d) MIP image of 3D-MRC using turbo-spin echo (TSE) shows the exact extent of tumor proximally and distally to the stenotic segment without image degradation by rotating MIP reconstructions. The reviewers judged that the overall image quality of 3D-MRC was higher than that of corresponding 2D thick section RARE and thin section RARE MRC.

Although the artifact of 3D-MRC was less than that of 2D-MRC, there was no statistical significance between 3D-MRC and 2D-MRC ($P > 0.05$)(Fig. 2). The reviewer 1 judged that the 2D HASTE had the most severe artifact.

For both reviewers, a highly significant ($P < 0.001$) ductal conspicuity was achieved with 3D-MRC imaging (Fig.3).

Figure 2. 69-year-old female with hilar cholangiocarcinoma (Bismuth type IV).





(a) 2D- thick section RARE image shows the tumor involvement of the hilar duct. (b) Axial fat suppressed T2-weighted image demonstrates a dilated right intrahepatic duct (black arrows). (c) Coronal T2-weighted image shows tumor involvement in the medial segment of left lobe (white arrows). The reviewers assessed that the tumor involved the right second confluence level and left second confluence of the bile duct was not invaded, which was classified into hilar cholangiocarcinoma, Bismuth type IIIa. (d)(e) MIP and source images of the 3D-MRC show the tumor involvement of the second confluence level of the left hepatic duct (white arrows) as well as right second confluence, which was classified into hilar cholangiocarcinoma, Bismuth type IV.

Figure 3. 86-year-old male with hilar cholangiocarcinoma (Bismuth type IV).



(a) 2D- thick section RARE image shows the tumor involvement of the hilar duct. (b) 2D-thin section multislice RARE image shows irregular narrowing of the left hepatic duct (arrow). The reviewers interpreted that the tumor was Bismuth type IIIa hilar cholangiocarcinoma. (c)(d) Rotating MIP images of the 3D-MRC reveal separation of the right anterior duct (short arrow) and right

posterior duct (long arrow) at the confluence level. The tumor seems not to extend to the second confluence of the left hepatic duct (arrow). Although the reviewers interpreted that the tumor did not involve the second confluence level of the left hepatic duct (Bismuth type IIIa), surgery and pathologic examination proved Bismuth type IV hilar cholangiocarcinoma. Because 3D-MRC using TSE has limitation in depicting the bile duct wall, the tumor extent was underestimated.

Extent of disease

To determine the tumor extent, hilar bile duct cancer (n=17) was divided into five types according to the Bismuth-Corlette classification²⁰, type I in one case, type II in 5 cases, type IIIa in 5 cases, type IIIb in 2 cases, and type IV in 5 cases. Extrahepatic bile duct cancers were divided into intrapancreatic and extrapancreatic cancers: intrapancreatic cancer in 2 cases, extrapancreatic cancer in 5 cases. Three patients had gallbladder cancers and the tumors invaded the right second confluence level corresponding to Bismuth-Corlette classification type IIIa. Three patients had periampullary tumors, and they were regarded as intrapancreatic CBD involvement. The patients with hilar bile duct cancer underwent right lobectomy (n=7), left lobectomy (n=3) or segmental resection (n=2). The patients with common bile duct cancer and periampullary tumors underwent segmental resection (n=6) or Whipple's operation (n=5). Palliative surgery was performed in eight patients.

The accuracy of the 2D-MRC and of the 3D-MRC for determining the classification of the tumor extent, is given in Table 2. The accuracy for determining the classification of the tumor extent at 2D-MRC was 67.7% (21 of 31 patients) for reviewer 1 and 70.9% (22 of 31 patients) for reviewer 2. The accuracy for determining the classification of the tumor extent at 3D-MRC was 74.1% (23 of 31 patients) for reviewer 1 and 77.4% (24 of 31 patients) for

reviewer 2. There was no statistical significance ($P= 0.091$ for reviewer 1 and $P=0.164$ for reviewer 2).

The accuracies with the 2D-MRC and of the 3D-MRC for evaluation of tumor extent for the two reviewers are given in Table 3. For right second confluence involvement, the Az values with 95% confidence intervals (CIs) of 2D- and 3D- images, were 0.989 (95% CI: 0.868, 1.000) and 0.964 (95% CI: 0.827, 0.995), respectively, for reviewer 1 and 0.922 (95% CI: 0.767, 0.986) and 0.998 (95% CI: 0.883, 1.000), respectively, for reviewer 2. There was no significant difference between the Az values of the 2D- and the 3D- MRC for both reviewers ($P = 0.431$ for reviewer 1 and $P = 0.126$ for reviewer 2). For left second order branch involvement, the Az values with 95% confidence intervals (CIs) of the 2D and 3D- images, were 0.890 (95% CI: 0.725, 0.972) and 0.943 (95% CI: 0.797, 0.992), respectively, for reviewer 1 and 0.917 (95% CI: 0.760, 0.984) and 0.813 (95% CI: 0.632, 0.929), respectively, for reviewer 2. There was no significant difference between the Az values of the 2D- and of the 3D-MRC for either reader ($P = 0.536$ for reviewer 1 and $P = 0.249$ for reviewer 2). For intrapancreatic CBD involvement, the Az values with 95% confidence intervals (CIs) of the 2D and 3D- images, were 0.732 (95% CI: 0.549, 0.878) and 0.737 (95% CI: 0.549, 0.878), respectively, for reviewer 1 and 0.798 (95% CI: 0.616, 0.920) and 0.707 (95% CI: 0.517, 0.856), respectively, for reviewer 2.

There was no significant difference between the Az values of the 2D- and of the 3D-MRC for either reader ($P = 0.955$ for reviewer 1 and $P = 0.186$ for reviewer 2).

The sensitivity, specificity, and accuracy of the tumor extent for reviewer 1 and 2, are given in Table 4. In right second order branch involvement, the accuracy of 2D-MRC for the two reviewers was 92.8%, 93.5%, respectively, and the accuracy of the 3D-MRC for the two reviewers was 96.7%, 96.7%, respectively. In left second order branch involvement, the accuracy of 2D-MRC for the two reviewers was 74.1%, 83.8%, respectively, and the accuracy of the 3D-MRC for the two reviewers was 93.5%, 87.0%, respectively. In intrapancreatic CBD involvement, the accuracy of 2D-MRC for the two reviewers was 77.4%, 80.6%, respectively, and the accuracy of the 3D-MRC for the two reviewers was 83.8%, 70.9%, respectively. The McNemar test revealed no significantly different sensitivities or specificities between 2D-MRC and 3D-MRC in regard to extent of disease ($P > .05$).

Table 2. Accuracy of 2D-MRC versus 3D-MRC for determining tumor extent according to the final diagnosis

Reviewer 1		Final Diagnosis	Reviewer 2	
2D-MRC	3D-MRC		2D-MRC	3D-MRC
3	4	Type II hilar cancer(5)	1	3
4	3	Type IIIa hilar cancer(5)	4	5
0	0	Type IIIb hilar cancer(2)	1	0
2	4	Type IV hilar cancer(5)	2	3
5	5	Extrapancreatic CBD cancer and type I hilar cancer (6)	5	5
5	5	Intrapancreatic CBD cancer and periampullary tumor (5)	5	5
2	2	Gallbladder cancer(3)	3	3
21	23	Total (31)	22	24

Data are numbers. Data in the parentheses are the number of patients.

Table 3. AUC (area under the curve) of extent of the disease according to the location

	2D MRC	3D MRC	P value
Right second order			
branch involvement			
Reviewer 1	0.989[0.868,1.000]	0.964[0.827,0.995]	0.431
Reviewer 2	0.922[0.767,0.986]	0.998[0.883,1.000]	0.126
Left second order			
branch involvement			
Reviewer 1	0.890[0.725,0.972]	0.943[0.797,0.992]	0.536
Reviewer 2	0.917[0.760,0.984]	0.813[0.632,0.929]	0.249
Intrapancreatic CBD			
involvement			
Reviewer 1	0.732[0.544,0.874]	0.737[0.549,0.878]	0.955
Reviewer 2	0.798[0.616,0.920]	0.707[0.517,0.856]	0.186
Overall tumor extent			
Reviewer 1	0.889[0.807,0.945]	0.903[0.823,0.954]	0.734
Reviewer 2	0.881[0.797,0.939]	0.864[0.791,0.935]	0.668

Note.- Data are values of Az. Numbers in brackets are 95% CI.

Table 4. Sensitivity, specificity, and accuracy of 2D-MRC and 3D-MRC according to the location of obstruction

			2D-MRC	3D-MRC
Right second order branch				
Reviewer 1	Sensitivity		92.8%(13/14)	100%(14/14)
	specificity		94.1%(16/17)	94.1%(16/17)
	Accuracy		93.5%(29/31)	96.7%(30/31)
Reviewer 2	Sensitivity		92.8%(13/14)	100%(14/14)
	specificity		94.1%(16/17)	94.1%(16/17)
	Accuracy		93.5%(29/31)	96.7%(30/31)
Left second order branch				
Reviewer 1	Sensitivity		28.5%(2/7)	85.7%(6/7)
	specificity		87.5%(21/24)	95.8%(23/24)
	Accuracy		74.1%(23/31)	93.5%(29/31)
Reviewer 2	Sensitivity		42.8%(3/7)	71.4%(5/7)
	specificity		95.8%(23/24)	91.6%(22/24)
	Accuracy		83.8%(26/31)	87.0%(27/31)
Intrapaneareatic CBD				
Reviewer 1	Sensitivity		44.4%(4/9)	66.7%(6/9)
	specificity		90.9%(20/22)	90.9%(20/22)
	Accuracy		77.4%(24/31)	83.8%(26/31)
Reviewer 2	Sensitivity		55.6%(5/9)	44.4%(4/9)
	specificity		90.9%(20/22)	81.8%(18/22)
	Accuracy		80.6%(25/31)	70.9%(22/31)

**Overall tumor extent including
right, left second order
branch, and intrapancreatic
CBD**

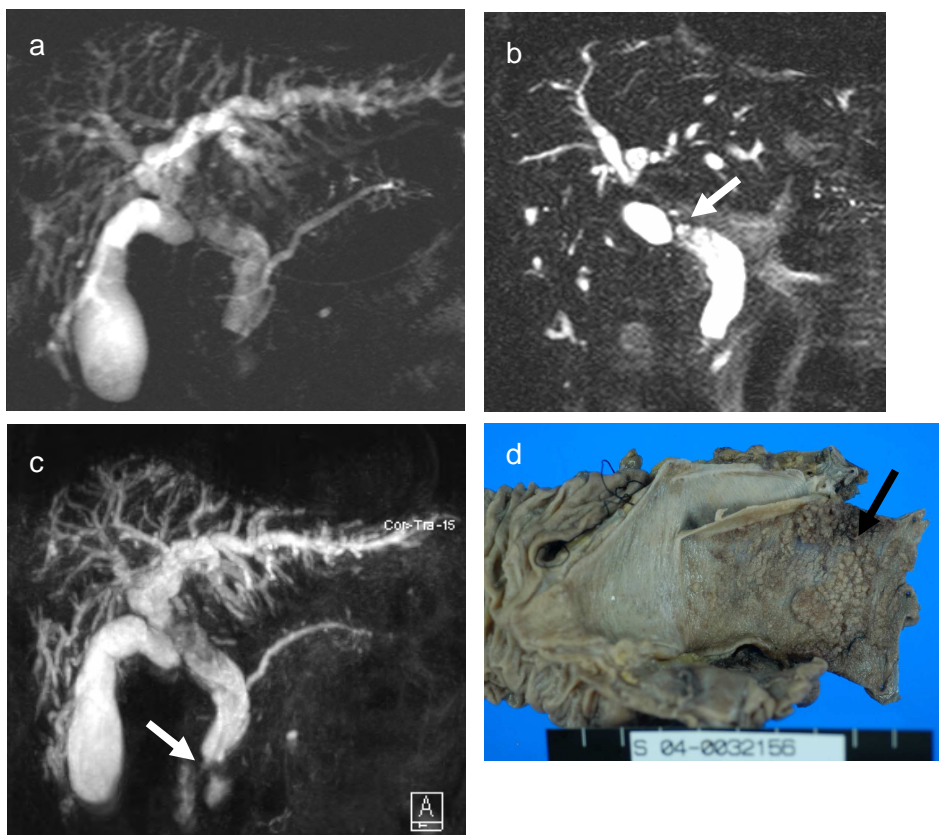
Reviewer 1	Sensitivity	73.3%(22/30)	86.7%(26/30)
	specificity	90.4%(57/63)	93.6%(59/63)
	Accuracy	84.9%(79/93)	91.4%(85/93)
Reviewer 2	Sensitivity	70.0%(21/30)	73.3%(22/30)
	specificity	93.6%(59/63)	90.4%(57/63)
	Accuracy	86.0%(80/93)	84.9%(79/93)

Data are percentages. Data in the parentheses are the number of patients.

Origin of tumors

The accuracy of determining the origin of tumors was 93.5% (29/31), 96.7% (30/31) for 2D-MRC and 83.8% (26/31), 87.1% (27/31) for 3D-MRC. Although 2D-MRC had higher accuracy in determining the origin of tumors, there was no statistical significance ($P=0.248$ for both reviewers) (Fig. 4).

Figure 4. 61-year-old male with papillary cholangiocarcinoma (Bismuth type II).



(a) 2D-thick section RARE image shows diffuse CBD and both IHD dilatation.

(b) Coronal fat suppressed T2-weighted image demonstrates the irregular intraluminal filling defect in the mid-CBD (arrow).

(c) MIP image of the 3D-MRC reveals the diffuse biliary dilatation. The reviewers interpreted that the tumor involved the intrapancreatic CBD (arrow). On retrospective review artifact of the source images led to false diagnosis by mimicking tumor involvement of the intrapancreatic CBD.

(d) Histopathologic examination depicts the papillary tumor in the mid CBD (arrow) without involvement of ampulla of Vater.

Interobserver agreement

Interobserver agreement between two sequences and the reviewers in the level of confidence in evaluation of tumor extent is given in Table 5. Substantial interobserver agreement is demonstrated for all sets without great variations between different techniques and the reviewers.

Table 5. Interobserver agreement in the level of confidence in evaluation of tumor extent

	κ Value
2D vs 3D for reviewer 1	0.757
2D vs 3D for reviewer 2	0.758
2D between reviewers	0.619
3D between reviewers	0.725*

* Weighted κ value

IV. Discussion

In my study, 2D-MRC and 3D-MRC had similar diagnostic accuracy in patients with malignant biliary obstruction. Although 3D-MRC has the tendency to show higher accuracy compared with 2D-MRC, no significant difference was observed in evaluating the disease extent of tumor for two sequences. However, 3D-MRC had superior image quality, ductal conspicuity to 2D-MRC.

MRC is a still evolving technique for the evaluation of biliary diseases. Two dimensional thick section single-shot RARE and multislice thin section half-Fourier RARE technique is being most commonly used for MRC, because of elimination of motion artifacts, high contrast-to-noise ratio, and increased spatial resolution compared with gradient echo-based T2-weighted sequences. The 2D thick section single-shot RARE technique has the major advantage of quickly acquiring an image giving an overview of ductal anatomy. The limitations of the thick section single-shot RARE are the lack of post-processing, resulting in the fact that individual tomographic section cannot be evaluated. Therefore thick section single-shot RARE technique alone is not suitable for the evaluation of the complex anatomical structures like hepatic hilum. Currently most institutes perform MRC using the combination of thick section imaging to provide an anatomical overview and thin section imaging to provide fine detail.

Although fat suppressed thin section half-Fourier RARE technique can be obtained with high speed and has the capability of MIP reconstruction, it has anisotropic resolution with increased slice thickness compared with in-plane resolution, resulting in marked degradation of MIP in planes oblique to the acquisition plane. The major advantage of 3D-MRC is that it provides isotropic MIP images without distortion. Therefore 3D-MRC could be used as complementary sequence to standard 2D-MRC in the evaluation of biliary tree.

Three-dimensional acquisition is appealing for MRC because it provides contiguous thin sections (approximately 1 mm in all three dimensions) that may be used to reconstruct images in any planes. Volumetric acquisition of a 3D-MRC have been used to improve the quality of MIP reconstruction using a variety of software to depict complex biliary ductal relationships^{2,15,19}. The increased spatial resolution of the 3D-MRC using TSE that was used for this study is reflected by a matrix of 320 X 320 pixels; the slice thickness was set to 1 mm, which minimize partial volume averaging. Although 3D-MRC failed to increase the diagnostic performance for the evaluation of tumor extent compared to 2D-MRC in our study, we expect the 3D-MRC have much to be improved in regard to spatial resolution and image quality with the continued advancement in MR technology including improved coil, higher SNR at 3T, and more sophisticated postprocessing software.

Image degradation by respiratory motion has been the greatest barrier to successful MRC. Breath-hold techniques and respiratory-triggered image acquisition have been applied to overcome this limitation. The recently introduced prospective acquisition correction (PACE) technique uses a real-time navigator sequence to monitor the movement of diaphragm which avoid magnetization saturation. The frequency of artifacts of the navigator-triggered TSE is reported to be lower than that of single-shot RARE sequence ^{21,22}. My study showed that navigator-triggered 3D-MRC using TSE has less artifacts than 2D-MRC; however there was statistically significant difference only in one reviewer.

Recent study reported that 3D-MRC using fast-recovery fast spin-echo is promising imaging technique for improving visibility of biliary tree, compared with the conventional 2D-MRC . Although 3D-MRC has the higher technical quality and overall image quality than 2D-MRC, there is still a limitation in improving the diagnostic performance for evaluating the extent of the disease in biliary obstruction. However, the high quality MIP reconstructions are very useful because they improve the understanding of complex anatomical structure like hepatic hilum by selecting the optimal viewing angle. In addition, MIP images also facilitate demonstration of the anatomical information to surgeons. I believe that 3D-MRC may be helpful for

preoperative planning in patients with hilar bile duct obstruction by showing the complex configuration more intuitively than 2D-MRC.

Two major disadvantages of 3D-MRC using TSE are long acquisition time and high level of background suppression which lead to low anatomical information regarding underlying parenchymal organs ²¹. The long acquisition time of 3D-MRC prevented its wide acceptance for biliary imaging in many institutes. Especially older patients with irregular breathing patterns require longer acquisition time than others and have tendency to show more artifact. A reduction of the acquisition time is feasible using parallel imaging technique. However, trade-off between image quality and acquisition time should be made in daily practice. The present study showed that 3D-MRC using TSE was inferior to the 2D images in regard to the origin of tumor because of background suppression, however there was no statistical significance.

My study has the following limitations: First, one possible bias was that because patients with potentially resectable disease undergo surgery, limiting our patient group to surgical patients would introduce a selection bias toward resectable disease. However, this selection bias might be reduced to some extent because the reviewers were informed that some patients who have hilar bile duct cancer invading bilateral second confluence underwent surgery for palliative purposes. Second, optimization of the 3D TSE sequence

parameters remains a work in progress. The decrease in acquisition time by using the parallel acquisition imaging could allow an increase in spatial resolution, although the decrease in signal-to-noise ratio would need to be evaluated.

V. Conclusion

In conclusion, 3D-MRC has superior image quality to 2D-MRC, however 3D-MRC showed no difference in accuracy compared with 2D-MRC for evaluating the extent of disease in patients with malignant biliary obstruction. 3D-MRC can be a complementary sequence to conventional 2D-MRC for the evaluation of biliary tree.

References

1. Schwartz LH, Coakley FV, Sun Y, Blumgart LH, Fong Y, Panicek DM. Neoplastic pancreaticobiliary duct obstruction: evaluation with breath-hold MR cholangiopancreatography. *AJR Am J Roentgenol* 1998;170(6):1491-1495.
2. Becker CD, Grossholz M, Mentha G, de Peyer R, Terrier F. MR cholangiopancreatography: technique, potential indications, and diagnostic features of benign, postoperative, and malignant conditions. *Eur Radiol* 1997;7(6):865-874.
3. Schofl R. Diagnostic endoscopic retrograde cholangiopancreatography. *Endoscopy* 2001;33(2):147-157.
4. Christensen M, Matzen P, Schulze S, Rosenberg J. Complications of ERCP: a prospective study. *Gastrointest Endosc* 2004;60(5):721-731.
5. Frey CF, Burbige EJ, Meinke WB, Pullos TG, Wong HN, Hickman DM, Belber J. Endoscopic retrograde cholangiopancreatography. *Am J Surg* 1982;144(1):109-114.
6. Fulcher AS, Turner MA, Capps GW, Zfass AM, Baker KM. Half-Fourier RARE MR cholangiopancreatography: experience in 300 subjects. *Radiology* 1998;207(1):21-32.
7. Varghese JC, Farrell MA, Courtney G, Osborne H, Murray FE, Lee MJ. A prospective comparison of magnetic resonance cholangiopancreatography with endoscopic retrograde cholangiopancreatography in the evaluation of patients with suspected biliary tract disease. *Clin Radiol* 1999;54(8):513-520.
8. Soto JA, Barish MA, Yucel EK, Siegenberg D, Ferrucci JT, Chuttani R. Magnetic resonance cholangiography: comparison with endoscopic retrograde cholangiopancreatography. *Gastroenterology* 1996;110(2):589-597.

9. Romagnuolo J, Bardou M, Rahme E, Joseph L, Reinhold C, Barkun AN. Magnetic resonance cholangiopancreatography: a meta-analysis of test performance in suspected biliary disease. *Ann Intern Med* 2003;139(7):547-557.
10. Hintze RE, Adler A, Veltzke W, Abou-Rebyeh H, Hammerstingl R, Vogl T, Felix R. Clinical significance of magnetic resonance cholangiopancreatography (MRCP) compared to endoscopic retrograde cholangiopancreatography (ERCP). *Endoscopy* 1997;29(3):182-187.
11. Mandler MH, Bouillet P, Sautereau D, Chaumerliac P, Cessot F, Le Sidaner A, Pillegand B. Value of MR cholangiography in the diagnosis of obstructive diseases of the biliary tree: a study of 58 cases. *Am J Gastroenterol* 1998;93(12):2482-2490.
12. Pavone P, Laghi A, Catalano C, Panebianco V, Fabiano S, Passariello R. MRI of the biliary and pancreatic ducts. *Eur Radiol* 1999;9(8):1513-1522.
13. Coakley FV, Schwartz LH. Magnetic resonance cholangiopancreatography. *J Magn Reson Imaging* 1999;9(2):157-162.
14. Sodickson A, Mortelet KJ, Barish MA, Zou KH, Thibodeau S, Tempany CM. Three-dimensional fast-recovery fast spin-echo MRCP: comparison with two-dimensional single-shot fast spin-echo techniques. *Radiology* 2006;238(2):549-559.
15. Barish MA, Yucel EK, Soto JA, Chuttani R, Ferrucci JT. MR cholangiopancreatography: efficacy of three-dimensional turbo spin-echo technique. *AJR Am J Roentgenol* 1995;165(2):295-300.
16. Wielopolski PA, Gaa J, Wielopolski DR, Oudkerk M. Breath-hold MR cholangiopancreatography with three-dimensional, segmented, echo-planar imaging and volume rendering. *Radiology* 1999;210(1):247-252.
17. Textor HJ, Flacke S, Pauleit D, Keller E, Neubrand M, Terjung B, Gieseke J, Scheurlen C, Sauerbruch T, Schild HH. Three-dimensional magnetic resonance cholangiopancreatography with respiratory

- triggering in the diagnosis of primary sclerosing cholangitis: comparison with endoscopic retrograde cholangiography. *Endoscopy* 2002;34(12):984-990.
18. Papanikolaou N, Karantanas AH, Heracleous E, Costa JC, Gourtsoyiannis N. Magnetic resonance cholangiopancreatography: comparison between respiratory-triggered turbo spin echo and breath hold single-shot turbo spin echo sequences. *Magn Reson Imaging* 1999;17(9):1255-1260.
 19. Soto JA, Barish MA, Alvarez O, Medina S. Detection of choledocholithiasis with MR cholangiography: comparison of three-dimensional fast spin-echo and single- and multisection half-Fourier rapid acquisition with relaxation enhancement sequences. *Radiology* 2000;215(3):737-745.
 20. Bismuth H, Nakache R, Diamond T. Management strategies in resection for hilar cholangiocarcinoma. *Ann Surg* 1992;215(1):31-38.
 21. Asbach P, Klessen C, Kroencke TJ, Kluner C, Stemmer A, Hamm B, Taupitz M. Magnetic resonance cholangiopancreatography using a free-breathing T2-weighted turbo spin-echo sequence with navigator-triggered prospective acquisition correction. *Magn Reson Imaging* 2005;23(9):939-945.
 22. Klessen C, Asbach P, Kroencke TJ, Fischer T, Warmuth C, Stemmer A, Hamm B, Taupitz M. Magnetic resonance imaging of the upper abdomen using a free-breathing T2-weighted turbo spin echo sequence with navigator triggered prospective acquisition correction. *J Magn Reson Imaging* 2005;21(5):576-582.

국문요약

악성 담관폐쇄 환자에서 2차원과 3차원 자기공명담관조영술의 비교

지도교수 김 명 진

연세대학교 대학원 의학과

최 진 영

본 연구의 목적은 악성 담관폐쇄 환자에서 2차원 자기공명담관조영술과 3차원 자기공명담관조영술을 비교하고자 함이다.

2004년 01월부터 2005년 10월까지 서울대학교 병원에서 악성 담관폐쇄로 진단되어 수술을 시행받고, 술전 2차원과 3차원 자기공명담관조영술을 시행한 31명의 환자를 대상으로 하였다. 환자들에 대하여 후향적으로 영상의 전반적인 질, 인공물, 담관의 선명도, 병변의 침범정도, 병변 침범에 대한 진단적 확신도, 종양의 기원에 대해 2명의 방사선과 의사가 평가하였고 이를 수술결과 및 병리학적 진단을 토대로 분석하였다.

3차원 영상이 2차원 영상에 비해 우수한 영상의 질을 보였다. 종양의 분류에 대한 정확도는 2차원 영상에서 67.7% (21/31)와 70.9% (22/31)였고 3차원 영상에서 74.1% (23/31)와 77.4% (24/31)로 유의

한 차이가 없었다. 2차원 영상과 3차원 영상에서 전체적인 종양의 침범 범위에 대한 Az값은 유의한 차이가 없었다 ($Az = 0.889, 0.881$ for 2D and $Az = 0.903, 0.864$ for 3D). 종양의 기원을 평가하는데 있어서도 2차원 영상과 3차원 영상간의 차이는 없었다 ($P > 0.05$).

3차원 자기공명담관조영술이 2차원 영상에 비해 영상의 질은 우수하였으나 두 기법은 악성 담관 폐쇄환자의 병변 범위를 평가하는데 있어서 유사한 진단능을 보인다.

핵심되는 말 : 자기공명담관조영술, 3차원, 악성 담관 신생물